Atmospheric
Chemistry
and Physics

Contributions of mobile, stationary and biogenic sources to air pollution in the Amazon rainforest: a numerical study with the WRF-Chem model

Sameh A. Abou Rafee[1], Leila D. Martins[1], Ana B. Kawashima[1], Daniela S. Almeida[1], Marcos V. B. Morais[1], Rita V. A. Souza[2], Maria B. L. Oliveira[2], Rodrigo A. F. Souza[2], Adan S. S. Medeiros[2], Viviana Urbina[3], Edmilson D. Freitas[3], Scot T. Martin[4], and Jorge A. Martins[1]

[1]Federal University of Technology – Parana, Londrina, Brazil
[2]Amazonas State University – Amazonas, Manaus, Brazil
[3]Department of Atmospheric Sciences, University of São Paulo, São Paulo, Brazil
[4]Harvard University, Cambridge, Massachusetts, USA

Correspondence to: Sameh A. Abou Rafee (samehabou@gmail.com) and Jorge A. Martins (jmartins@utfpr.edu.br)

Abstract. This paper evaluates the contributions of the emissions from mobile, stationary and biogenic sources on air pollution in the Amazon rainforest by using the Weather Research and Forecasting with Chemistry (WRF-Chem) model. The analyzed air pollutants were CO, NO_x, SO_2, O_3, $PM_{2.5}$, PM_{10} and volatile organic compounds (VOCs). Five scenarios were defined in order to evaluate the emissions by biogenic, mobile and stationary sources, as well as a future scenario to assess the potential air quality impact of doubled anthropogenic emissions. The stationary sources explain the highest concentrations for all air pollutants evaluated, except for CO, for which the mobile sources are predominant. The anthropogenic sources considered resulted an increasing in the spatial peak-temporal average concentrations of pollutants in 3 to 2780 times in relation to those with only biogenic sources. The future scenario showed an increase in the range of 3 to 62 % in average concentrations and 45 to 109 % in peak concentrations depending on the pollutant. In addition, the spatial distributions of the scenarios has shown that the air pollution plume from the city of Manaus is predominantly transported west and southwest, and it can reach hundreds of kilometers in length.

1 Introduction

The impacts of anthropogenic emissions from urban areas on the environment and human health have been covered in several scientific studies through different methodologies (Kampa and Castanas, 2008; Martins et al., 2010). These analyses have shown that the consequences of such emissions go beyond their initial source and can reach even farther during long periods. In general, most recent studies focus mainly on the aftermath of the anthropogenic emissions from the megacities in the developing world (e.g., Zhu et al., 2013). This has happened because such cities have increased their energy demand, which has been high throughout recent decades (Lutz et al., 2001). For instance, energy consumption in China has increased more than 300 million tons of coal equivalent (MtCE), compared to the previously amount of 1349 MtCE. Most of this energy is produced from burning fossil fuels, mainly coal (Crompton and Wu, 2005). As a consequence, the atmosphere in these regions has experienced a great increase not only in particles but also in gases such as carbon monoxide (CO), sulfur dioxide (SO_2), nitrogen oxides (NO_x), and other secondary compounds such as ozone (O_3). Understanding the predominant sources of each pollutant is key to designing successful regulatory policies to improve air quality and bring benefits to public health.

Determining what is the real contribution of the anthropogenic air pollutants to the environment and to human health is not a straightforward task. Its difficulty lies in separately studying the emissions from natural and human sources and their complex combination. Although urban areas can have an identity associated with their economic profile, the transport and interactions of atmospheric pollutants effects hamper the understanding of the role of each emission species in the studied region. In this context, atmospheric models with an explicit treatment of the physical and chemical processes become an indispensable tool to the studies of the urban pollution impact. Several numerical studies can be found with special focus on different aspects of the pollution impact, such as pollution episodes (Jiang et al., 2012; Michael et al., 2013; Kuik et al., 2015), regional and long-distance transport (Tie et al., 2007; Guo et al., 2009; Lin et al., 2010), secondary formation of gases and particles (Yerramile et al., 2010; Jiang et al., 2012; Lowe et al., 2015), and the effects of land use and land cover changes (Capucim et al., 2015; Rafee et al., 2015). However, such studies did not investigate the impact of isolated urban plumes.

The pronounced growth of urban areas in recent decades, mainly due to the accelerated population growth rate and the migratory flow to cities, resulted in a few areas in the world where an isolated urban area would interact with an environment of natural and homogeneous characteristics. The city of Manaus is one of the unique scenarios in the world where an isolated urban area is in the center of a vast tropical forest area, the Amazon rainforest (Martin et al., 2016). Thus, the region is a valuable laboratory, for example for studying the impact of anthropogenic emissions of air pollutants on atmospheric chemical composition. Although there are a number of studies involving the measurements of atmospheric pollutants in the Amazon region (e.g., Kuhn et al., 2010; Trebs et al., 2012; Baars et al., 2012; Artaxo et al., 2013), most of the contribution was published very recently with the results of the GoAmazon2014/5 project (Martin et al., 2016, 2017; Alves et al., 2016; Pöhlker et al., 2016; de Sá et al., 2017; Kourtchev et al., 2016; Hu et al., 2016; Bateman et al., 2017; Cecchini et al., 2016; Jardine et al., 2016). In terms of numerical studies, only a few studies focusing the role of the anthropogenic emission sources in urban areas are available (Freitas et al., 2006; Andreae et al., 2012; Beck et al., 2013; Bela et al., 2015). These studies do not address the participation of each type of emission source on air pollutants, which is important for the formulation of regulatory public policies for air quality management. This type of evaluation can only be performed with the use of atmospheric modeling tools, which require the preparation of an inventory for mobile and stationary sources, since no official and public emissions inventory is available for Manaus.

Given the importance of anthropogenic emissions in the Amazon region, this paper reports a numerical study evaluating the impact of the urban pollution plume on pollutant concentrations above the preserved forest region considering individual contributions from the main mobile and stationary sources in Manaus. In addition, a companion study by Medeiros et al. (2017) focuses on how the changing energy matrix for power production affects air quality in the Manaus region. Both studies were conducted using the Weather Research and Forecasting with Chemistry (WRF-Chem) model, where the simulations for diverse scenarios were performed according to the current conditions of the region. The numerical experiments performed in this work addressed the following issues:

- participation of mobile and stationary anthropogenic sources and biogenic sources in the concentration of trace gases and particles for the city of Manaus and adjacent areas directly influenced by it;

- preferential direction and the distance of the urban plume impact from Manaus in the Amazon region;

- impact on air quality due to the likely future increase in anthropogenic emissions from mobile and stationary sources.

2 Methodology

2.1 Area and period of study

The region of the study comprises the urban area of Manaus and its surroundings, with a total area of $230\,560\,\mathrm{km}^2$ (Fig. 1). Manaus is located in northern Brazil, at latitude $3°06'07''$ and longitude $60°01'30''$ with an urban area of $377\,\mathrm{km}^2$, presented in the center of the simulated grid. Currently, Manaus has an estimated population of 2 million people, representing more than 50 % of the population in the state of Amazonas, with 99.49 % of its population living in urban areas (IBGE, 2014).

The simulation period encompasses the dates of 16–18 March 2014, and this period is part of the rainy season in the region (Fisch et al., 1998). Due to the scarce availability of air quality data, the choice of the days for simulations was made according to that availability, which is necessary to evaluate the performance of the model with the observed ground-based data. Four measurement sites of meteorological variables and air pollutants concentrations were available in different locations in the study area, as presented in Fig. 1: T1, located within the city of Manaus, at the National Institute for Amazonian Research (INPA); T3, located in the north of Manacapuru, approximately 100 km from Manaus, at stations of the project Green Ocean Amazon (GoAmazon2014/5); Colégio Militar and Federal Institute of Amazonas (IFAM), located in the city of Manaus; and a fourth site associated with the Project REMCLAM Network of Climate Change Amazon from the University of the State of Amazonas (UEA). According to the data from stations located in the city of Manaus, there was no record of rainfall within the given period, whereas the Manacapuru site
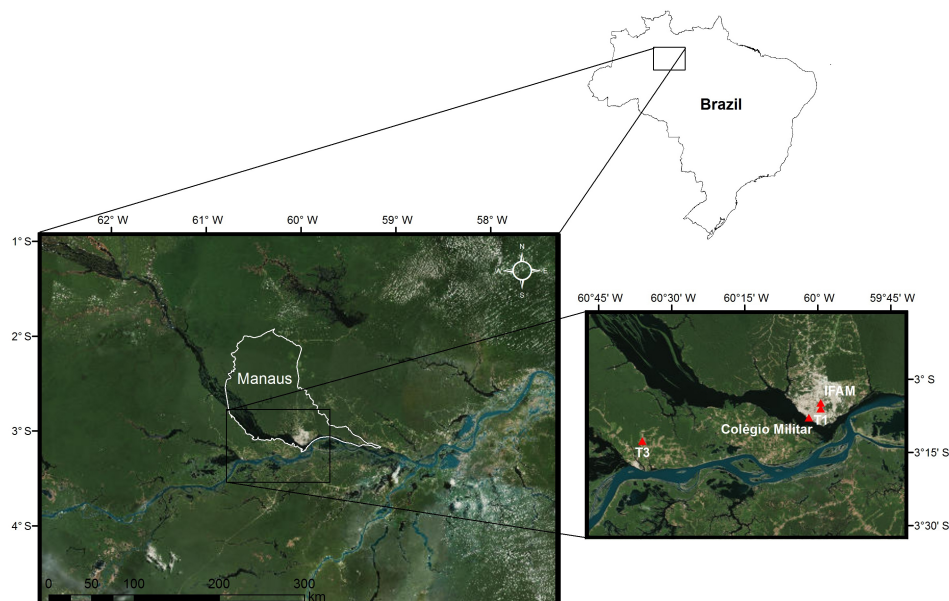
Figure 1. Geographic location of the study area, meteorology stations (Colégio Militar, IFAM and T3) and air quality station (T1). The white contour line shows the delimitation of the city of Manaus.

recorded 7.2 mm rainfall. Regarding the predominant wind direction, the ground-based data observed a prevalence of winds from the north, northeast and east. Figure S1 of the Supplement shows a time evolution of streamlines and the potential temperature advection, where these atmospheric conditions can be seen. In terms of wind direction climatology, the prevailing northeasterly/westerly winds blow all year round, 10–60° azimuth (November to March) and 90–130° azimuth (May to September) (Araújo et al., 2002). Another important factor when choosing the period of study was the low incidence of biomass burning wildfires in the rainy season. Fire outbreaks in the Amazon region are predominant during the dry season and can therefore affect the concentration of particulate matter and trace gases (Andreae and Merlet, 2001; Martins and Silva Dias, 2009). Since the purpose is only to analyze the impact of anthropogenic emissions attributed to fossil fuels, periods with the presence of regional wildfires would not be ideal.

2.2 Model description

In this study, the coupled WRF-Chem (Weather Research and Forecasting with Chemistry; Grell et al., 2005) model, version 3.2, was applied. The model is an online system that simultaneously predicts meteorological and chemical states. WRF/Chem or its previous versions have been applied in a large number of studies worldwide (e.g., Grell et al., 2005; Wang et al., 2009, 2010; Tuccella et al., 2012; Vara-Vela et al., 2015). The physical options (Table 3) used were defined according to the recent options inserted in the model, as well as those already tested in simulations by other works (e.g.,

Table 1. WRF-Chem physics parametrizations used for this study.

Process	Reference
Microphysics	Milbrandt and Yau (2005)
Surface layer	MM5 (Zhang and Anthes, 1982)
Soil–land parameterization	Noah LSM (Chen and Dudhia, 2001)
Boundary layer	YSU (Hong and Dudhia, 2003)
Shortwave radiation	Dudhia (Dudhia, 1989)
Longwave radiation	RRTM (Mlawer et al., 1997)

Vara-Vela et al., 2016). Furthermore, some combinations of physical parametrizations were tested and the combination that best represented the meteorological parameters observed (temperature and relative humidity) was used.

For the biogenic emission, the module used was based on descriptions by Guenther et al. (1993, 1994), Simpson et al. (1995) and Schoenemeyer et al. (2007). This module deals with isoprene, monoterpenes, volatile organic compound (VOC) emissions and emissions of nitrogen from the soil. Biogenic emissions were calculated using the categories of land use available in the model in which emission rates are estimated from the temperature and photosynthetic active radiation, which is the fraction of solar radiation comprised in the range of the visible spectrum available (0.4 to 0.7 µm) for the photosynthesis process. The aerosol parameterization used was based on the Modal Aerosol Dynamics model for Europe (MADE; Ackermann et al., 1998), developed from the Regional Particulate Model (RPM; Binkowski and Shandar, 1995), embedded with the representation of or-

ganic aerosol from the Secondary Organic Aerosol Model (SORGAM, developed by Schell et al., 2001).

For the gas-phase chemistry, the chemical mechanism used was the Regional Acid Deposition Model version 2 (RADM2; Chang et al., 1989), originally developed by Stockwell et al. (1990). RADM2 is widely used in atmospheric models to predict concentrations of oxidants and other pollutants and contains 158 chemical reactions, of which 21 are related to photolysis.

The simulation domain was configured with a 3 km horizontal grid spacing, with 190 grid points in x and 136 grid points in y directions, centered in the city of Manaus (3°4′12″ S, 59°59′24″ W). In the vertical grid, 35 levels were defined, with the top of the model at 50 hPa, corresponding to about 20 km in height above the mean sea level. Analysis data from the Global Model Data Assimilation System (GDAS), with a horizontal grid spacing of 1° and 26 vertical levels were used for initial and boundary conditions of the meteorological variables. For chemical variables, the initial and boundary conditions of simulations consist of idealized, northern hemispheric, mid-latitude, clean environmental conditions as described in Liu et al. (1996) and applied in studies such as those conducted by Grell et al. (2005), Wang et al. (2009, 2010), Tuccella et al. (2012) and Vara-Vela et al. (2016). On the other hand, there are studies where the chemical compound profiles used as initial and boundary conditions were based on anthropogenic emission inventories, including CO, NO$_x$, SO$_2$, speciated VOC, black carbon (BC), organic carbon (OC), and particulate material (PM), at 0.5° × 0.5° (e.g., Zhang et al., 2009) or higher resolutions (e.g., Tie et al., 2010). Initial and boundary conditions for chemical species have also been extracted from the output of global chemical transport models, such as the Model for OZone And Related chemical Tracers (MOZART; Hu et al., 2010). However, it is important to evaluate the global model results before deciding which global model to use in order to provide the chemical initial and boundary conditions, considering that there are many uncertainties among the global results.

Different times to avoid a spin-up effect are suggested in the literature, with values of 12 (Tuccella et al., 2012; Carvalho et al., 2015), 24 (Wang et al., 2009), 36 (Hu et al., 2010), and 48 h (Tie et al., 2010) of simulation as a model spin-up. There are also studies considering a few days as a model spin-up (e.g., Wang et al., 2010). In this study, a 24 h spin-up time was considered. For land use, spatial data from the Moderate-resolution Imaging Spectroradiometer (MODIS) 2005 file were utilized, with 500 m grid spacing (Schneider et al., 2009).

2.3 Anthropogenic emission inventories

2.3.1 Vehicle emissions

Emissions of all classes of light-duty and heavy-duty vehicles in the study region were taken into consideration for mobile sources. In order to calculate the emissions of air pollutants, information was collected based on the estimate of the number and type of vehicles, emission factors and average vehicle-use intensity. The calculations included individual contributions of five types/fuel combinations of vehicles (Table 2), considering the data estimated from the Brazilian National Department of Traffic (DENATRAN, 2014) for the city of Manaus. The urban area of Manaus contains 83.22 % of the vehicles in the state of Amazonas, corresponding to over 600 000 vehicles in the current fleet. Therefore, the fraction of the vehicle fleet according to type and fuel consumption for the entire study grid was considered based on data from Manaus. The fractions corresponding to light-duty vehicles using gasohol (a mixture of gasoline and ethanol ranging between 20 and 25 % of anhydrous ethanol), ethanol and flex fuel represent 22.81, 2.49 and 42.29 %, respectively. Heavy-duty diesel-powered vehicles represent 8.8 %, and motorcycles using gasohol represent 23.61 %.

The emission factors for different vehicle types/fuel assumed in the calculations were based on experiments conducted inside the road traffic tunnels in the city of São Paulo (Martins et al., 2006; Sánchez-Ccoyllo et al., 2009; Brito et al., 2013), which are the only vehicle emission factor measurements available in Brazil. The values were adopted for CO, NO$_x$, SO$_2$, and particulate matter (PM) as well as the distribution of VOC emission fractions related to evaporative, liquid and exhaust emissions for vehicles burning gasohol, ethanol and diesel. These values correspond to those that have been recently used in the study by Andrade et al. (2015) and are listed in Table 2. Based on these emission factors, diurnal profiles using hourly variations for emissions of trace gases and PM were used in the model (Martins et al., 2006; Andrade et al., 2015). The distribution of the fractionation of emission of fine particulate matter, as well as the chemical characterization, was obtained based on several studies in the city of São Paulo for the measurements of the concentration mass and number of particulate matter (Ynoue and Andrade, 2004; Miranda and Andrade, 2005; Albuquerque et al., 2011), and are used in the investigations by Andrade et al. (2015) and Vara-Vela et al. (2015).

In order to calculate the vehicle-use intensity, reference estimates from the first Brazilian National Emissions Inventory of Road Motor Vehicles (MMA, 2011), DENATRAN and the Brazilian National Agency of Petroleum (ANP, 2014a) were used. The intensities for light-duty vehicles, heavy-duty vehicles and motorcycles are 21.3, 128.4 and 70.6 km per day, respectively.

The spatial distribution of the number of vehicles in each grid point was based on nighttime lights from

Table 2. Emission factors for CO, NO_x, PM, SO_2, and VOCs, in grams per kilometer, for different vehicle type–fuel combinations.

Vehicle type	Fuel burned	CO	NO_x	PM	SO_2	VOCs (evaporative)	VOCs (liquid)	VOCs (exhaust)
Light-duty vehicles	Gasohol	5.43	0.34	0.15	0.03	0.17	2.00	1.24
	Ethanol	12.00	1.12	0.15	0.01	0.04	1.50	2.12
	Flex	5.13	0.32	0.15	0.02	–	–	0.15
Heavy-duty vehicles	Diesel	4.95	9.81	0.44	0.61	–	0	2.48
Motorcycles	Gasohol	9.15	0.13	0.05	0.01	–	1.40	2.37

the Defense Meteorological Satellite Program's Operational Linescan System (http://ngdc.noaa.gov/eog/dmsp/downloadV4composites.html), considering the size of urban occupation. Martins et al. (2008) have described this approach, which has performed a luminance calibration according to the population density and number of vehicles, presenting a good correlation between the parameters.

2.3.2 Stationary source emissions

The emission of thermal power plants (TPPs) of different types of fuel burning have been considered for the inventory of stationary sources in the studied region and the refinery located within the urban area of Manaus. It is noteworthy that the contributions of the industries located within the urban area have little significance in the region, due to the production concentrated mainly in transport and communication areas such as electronics, metal mechanical sectors and the production of motorcycles (MANAUS, 2002). In this case, the contributions on anthropogenic emissions occur indirectly by the high consumption of electricity supplied by the TPPs. The emission of the pollutants per type of TPP in each grid point of study has been calculated according to the estimates of emission factors, fuel consumption and power generation, using Eq. (1):

$$E_{p(i,j)} = \sum_{k=1}^{N} EF_P \times FC \times PG_{(i,j,k)}, \qquad (1)$$

where $E_{p(i,j)}$ represents the emission of pollutant P at each grid point (i, j), in grams per hour $(g\,h^{-1})$; EF_P is the emission factor of pollutant P, in grams per liter $(g\,L^{-1})$; FC is the fuel consumption, in liters per kilowatt hour $(L\,kWh^{-1})$; and $PG_{(i,j,k)}$ is the power generation of TPP (k) at each grid point (i, j) m in kilowatt (kW).

According to the Generation Database (BIG) of the National Electric Energy Agency (ANEEL, 2014), Brazil has 1890 TPPs in operation, with a total installed capacity of about 37.8 GW. Based on the information contained in BIG, a spatial distribution of TPPs has been performed at each grid point of the study area, with 59 diesel, 6 fuel oil and 8 natural gas power plants (Fig. 2) found in the grid, generating a power of 1851 MW, corresponding to 96.76 % of all gen-

eration in the state of Amazonas. The other TPPs located in state are very small.

Due to several types of technologies used in the burning fuels of TPPs, the emission factor admitted in the calculation was the intermediate values between the lower and upper limits adopted by the US Environmental Protection Agency (EPA, 1998, 2010), which has a complete estimation of emission factor for all air pollutants simulated. The emission factors are described in Table 3, and for comparative purposes, the values adopted in the inventory of São Paulo Environmental Protection Agency (CETESB, 2009) have also been listed. The distribution of PM has been done based on the fractionation designed for vehicle emissions. In addition, the speciation of VOC emissions have been performed for each TPP fuel type estimated by EPA (1998, 2010). Regarding the average fuel consumption for each type of TPP, the average value of fuel to produce 1 kWh of power has been adopted as described in the annual report of isolated operation systems for the North region (ELETRO-BRAS, 2013). For fuel oil, diesel and natural gas, the values of $0.27\,L\,kWh^{-1}$, $0.29\,kg\,kWh^{-1}$ and $0.28\,m^3\,kWh^{-1}$, respectively, have been considered.

Some approximations that were assumed to obtain the emission factor values of Table 3 were as follows:

- Fuel with 1 % sulfur content was assumed to calculate the emission factor of SO_2.

- Total organic compounds (TOCs) include VOCs, semi-volatile organic compounds, and condensable organic compounds.

- For NO_x emissions by fuel oil power plants, the minimum value was attributed to the lowest value available for vapor generation above $50\,t\,h^{-1}$ and the maximum value was assigned to the greatest value available for plants below $50\,t\,h^{-1}$.

- For the emission factors attributed to SO_2 and PM, the minimum and maximum values were defined based on the grade of fuel burned. In this case, the combustion of lighter distillate oils results in significantly lower PM formation than those from the combustion of heavier residual oils. According to the values proposed by EPA,
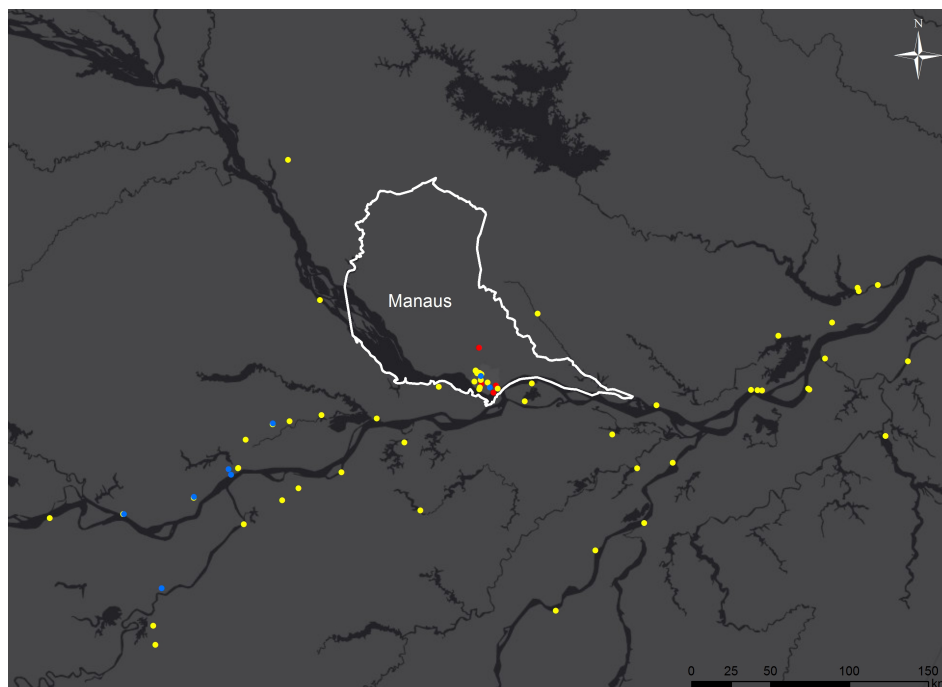
Figure 2. Spatial distribution of diesel (yellow), fuel oil (red) and natural gas (blue) TPPs on the study grid, and the border of Manaus (white).

burning no. 4 or no. 5 oil usually produces less SO_2 and PM than the burning of heavier no. 6 oil.

Brazil has 17 petroleum refining units with a production of about 769 million m^3 of petroleum per year (ANP, 2014b), with only one unit located in the North region, on the banks of the Rio Negro in Manaus (located at latitude $\lambda = 3°08'47''$ and longitude $\varphi = 59°57'15''$) – the Issac Sabbá refinery (REMAN). The total emission of each pollutant of the refinery is given by Eq. (2):

$$E_{p(i,j)} = EP_p \times V, \tag{2}$$

where $E_{p(i,j)}$ represents the emission of the pollutant P, in grams per hour ($g\,h^{-1}$), EP_p is the emission factor of pollutant P in grams per liter ($g\,L^{-1}$) and V is the volume of refined petroleum in liters per hour ($L\,h^{-1}$).

According to the National Petroleum Agency (ANP, 2014b), REMAN has as average production of approximately 1.7×10^6 L of petroleum per hour. The emission factors of the pollutants have been admitted from Presidente Bernardes Refinary (RPBC), located in Cubatão, São Paulo, Brazil. The VOC speciation profiles used have also been obtained from the EPA (1990).

The total emissions for CO, NO_x, SO_2, PM and VOCs for the stationary and mobile sources that represent the C0 scenario are shown in Table S1 in the Supplement. These results demonstrate that global inventories underestimate mobile and stationary sources in Manaus. For instance, in the MAC-City anthropogenic emissions inventory (MACCity, 2014),

the approximate sums of emissions in the study grid were $0.011\,Tg\,yr^{-1}$ (versus 0.068 in this study), $0.003\,Tg\,yr^{-1}$ (versus 0.087 in this study), $0.002\,Tg\,yr^{-1}$ (versus 0.073 in this study) for CO, NO_x and SO_2, respectively. For example, Fig. 3 shows the contribution, in percent, of NO_x and SO_2 emissions from all anthropogenic sectors considered.

2.4 Numerical scenarios

The investigations were defined by five numerical experiments (Table 4) to the study of the influence of mobile and stationary emissions in the region, which are as follows:

- Scenario C0: considering the main sources in the region (biogenic natural emission, vehicle, TPPs and REMAN refinery) representing the emission inventory of current conditions of the region.

- Scenario C1: numerical experiment with only biogenic natural emission, which simulates an atmospheric condition of an environment without the interference of human activities.

- Scenario C2: simulation with natural and vehicular emissions, intended to evaluate how the anthropogenic emissions characterized on solely vehicular sources affect the atmospheric chemistry.

- Scenario C3: considering natural and TPPs and refinery anthropogenic emissions, aimed at assessing the impact of stationary sources on air pollutant emissions.

Table 3. Emission factors of TPPs per fuel type.

Fuel type Pollutant	Natural gas ($g\,10^6\,L^{-1}$) EPA	CETESB	Fuel oil EPA	($g\,L^{-1}$) CETESB	Diesel EPA	($g\,L^{-1}$) CETESB
CO	384–1568	–	0.6	–	4.9–2.4	–
PM	121.6	48–219	0.05–1.2	0.84–1.45	0.59–1.6	0.24
NO_x	512–4480	2240–8800	1.2–6.6	6.6–8	18.3–54.1	2.4
SO_2	9.6	9.6	17–18.8	18.2–19.2	5.8–18.2	17.2
TOCs	176	28–92	0.03–0.3	0.03–0.13	0.04–1.6	0.03

Source: EPA, AP-42 (1998, 2010); CETESB (2009).
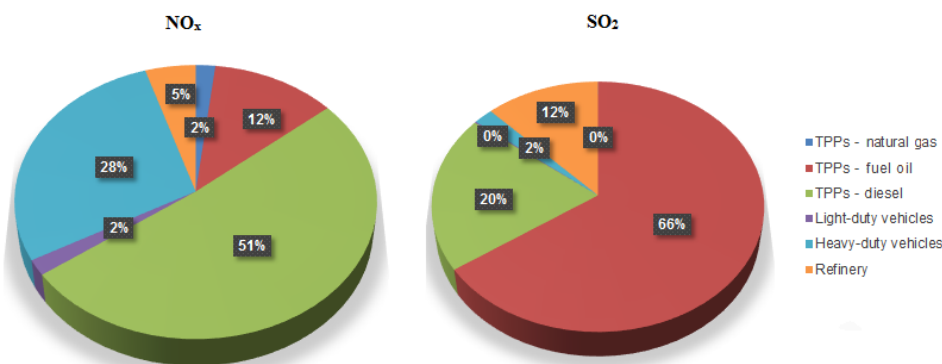
Figure 3. NO_x and SO_2 emission contribution from all anthropogenic sectors considered.

– Scenario C4: simulation including natural and twice the mobile and stationary emission sources, and twice the urban area of Manaus, which aimed at simulating an environment presenting a growth of the regional population and urban area, as well as increased anthropogenic emissions. The urban expansion has been concentrated in the agricultural and forest areas, preserving the water resources, as well as forest reserves and parks around the city of Manaus.

The meteorological fields and air pollutants obtained from the simulation of scenario C0 have been compared to the ground-based data observed (see Fig. 1). The analysis of meteorological variables has been conducted based on Pielke's skill score (S_{pielke}) (Pielke, 2002; Hallak and Perreira Filho, 2011), Pearson's correlation coefficient (r), and mean bias (MB). For the air pollutants, in addition to r and MB, two statistical indexes were used, the mean normalized bias error (MNBE) and the mean normalized gross error (MNGE). Such parameters have often been used in several studies to assess the performance of atmospheric models (e.g., Tie et al., 2007; Han et al., 2009; Tuccella et al., 2012). Table 5 shows a summary of the statistical indexes used to evaluate the model performance.

3 Results

3.1 Evaluation of the baseline scenario

3.1.1 Meteorology

Figure 4 shows the comparison between the observed and the simulated values for temperature and relative humidity at Colégio Militar, IFAM, T1 and T3, corresponding to the periods of 17–18 March 2014. Overall, there is a good representation of the temporal evolution of the temperature (e.g., $r = 0.91$ for T1) both for the average value and the daily minimum. The T1 station has the highest peak of temperature: about $36\,^\circ C$, which is the highest among the monitoring points compared to simulations. However, the model has proven to present difficulties in simulating the maximum temperature, mainly for T1 station, which is located in the central part of the urban area of Manaus. For the IFAM station, which is also a central site, diurnal peak (e.g., $33.5\,^\circ C$ average observed compared to $30.3\,^\circ C$ simulated at 14:00 LT) and minimum night (e.g., $24.8\,^\circ C$ average observed compared to $26.3\,^\circ C$ simulated at 02:00 LT) temperatures were weakly represented. For all stations, the model presents problems in capturing the peak temperature. The relative humidity profiles show a good level of agreement of the simulation to the average values of Colégio Militar ($r = 0.89$ and RMSE = 5.1) and T1 ($r = 0.88$ and RMSE = 4.8). However, sites IFAM and T3 have the greatest discrepancies

Table 4. Summary of simulation scenarios.

Scenarios	Emissions
C0	Biogenic, vehicular and stationary (TPPs and REMAN refinery) sources
C1	Only biogenic sources
C2	Biogenic and vehicular
C3	Biogenic and stationary (TPPs and REMAN refinery) sources
C4	Biogenic and doubled mobile and stationary sources

Table 5. Statistical indexes used to evaluate the model performance.

Indexes	Equation*
Pearson's correlation coefficient	$r = \dfrac{\sum\limits_{k=1}^{N}(p_k - \bar{p})(o_k - \bar{o})}{\left[\sum\limits_{k=1}^{N}(p_k - \bar{p})^2\right]^{1/2}\left[\sum\limits_{k=1}^{N}(o_k - \bar{o})^2\right]^{1/2}}$
Mean bias	$\text{MB} = \dfrac{1}{N}\sum\limits_{k=1}^{N}(p_k - o_k) = \bar{p} - \bar{o}$
Root mean square error	$\text{RMSE} = [\dfrac{1}{N}\sum\limits_{k=1}^{N}(p_k - o_k)^2]^{1/2}$
Pielke skill	$S_{\text{Pielke}} = \left|1 - \dfrac{\sigma_p}{\sigma_o}\right| + \dfrac{\text{RMSE}}{\sigma_o} + \dfrac{\text{RMSE} - \text{bias}}{\sigma_p}$
Mean normalized bias error	$\text{MNBE} = \dfrac{1}{N}\sum\limits_{k=1}^{N}\left[\dfrac{(p_k - o_k)}{o_k}\right] \times 100$
Mean normalized gross error	$\text{MNG} = \dfrac{1}{N}\sum\limits_{k=1}^{N}\left[\dfrac{|p_k - o_k|}{o_k}\right] \times 100$

* p_k and o_k are the predicted and observed value at time k, respectively.

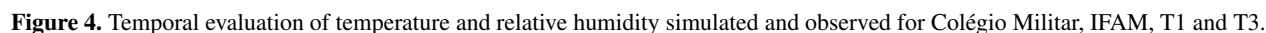among the results, with MB values equal to -8.3 and -10.1, respectively.

Regarding the statistical indexes presented in Table 6, the correlation coefficient (r) has provided satisfactory results for all stations, with the lowest values for temperature (0.87) and humidity (0.71) associated with T3 station and the highest values of 0.91 and 0.89 for Colégio Militar, respectively. According to Pielke's parameter skill defined in Hallak and Pereira Filho (2011), a good model performance occurs for index values of less than 2. In this case, the performance of the model is satisfactory for most of the stations, except for temperature at T1 ($S_{\text{pielke}} = 2.9$) and relative humidity at IFAM ($S_{\text{pielke}} = 3.7$) and T3 ($S_{\text{pielke}} = 3.9$). According to the mean bias, it has been observed that the simulation, in general, underestimates the majority of observed values, mainly for temperature (T1, MB $= -1.5$) and relative humidity (IFAM, and T3).

3.1.2 Air pollutants

T1 is the only station that has air quality data and only for NO_x, CO and $PM_{2.5}$ concentrations. Figure 5 and Table 7 show the comparisons between the simulation (scenario C0) and the observation of such pollutants. In terms of the $PM_{2.5}$, it has been observed, in general, that the model tends to over-

estimate the values observed (MNBE $= 50.8$), whereas with CO and NO_x the tendency is the opposite. They underestimated the values in most of the simulation period (MNBE equal a -29.5 and -35.4 for NO_x and CO, respectively). The most significant differences have been observed during the peak hours and mainly for CO. The weakest performance of the model happens mainly during the nocturnal peak, situated generally between 18:00 and midnight (local time). A possible explanation for the poor performance of the model during nocturnal peaks of CO is the fact that the fire outbreaks were not considered (four spots of fire occurred during the period inside the grid, although a low incidence of fire outbreaks was the criterion used for chosen the simulation period, Fig. S2), which could have influenced the simulated values. The MB indicates that the three analyzed pollutants present significant differences, with the value of $PM_{2.5}$ MB of $1.30\,\mu\text{g m}^{-3}$ compared to a $0.66\,\mu\text{g m}^{-3}$ average observed, NO_x with values of -26.2 ppb compared to an 88.7 ppb average observed, and CO presenting -135 ppb of MB compared to a 382.6 ppb average observed. Similar to the Pearson coefficient, the model shows good correlations for $PM_{2.5}$, NO_x and CO with 0.72, 0.53 and 0.53, respectively. In addition, in order to assess the sensitivity of the model to respond to different emission scenarios, numerical experiments were

Figure 4. Temporal evaluation of temperature and relative humidity simulated and observed for Colégio Militar, IFAM, T1 and T3.

carried out considering variations in emissions of ± 15 and $\pm 30\%$ in relation to scenario C0 (biogenic natural emission + vehicle + thermal power plants + REMAN refinery). Temporal evolution of PM_{10} and NO_x concentrations is shown in Fig. S3. Overall, it was observed that the model is sensitive to the variations performed and for PM_{10} and NO_x the responses to the variations are linear. However, O_3 changes are not linear to emission variations in VOC and NO_x (Atkinson, 2000; Martins and Andrade, 2008).

There are a few studies measuring the impact of the urban plume of Manaus on the pollutant concentration downwind of the city. For example, CO concentrations of 90–120 ppb were observed by Martin et al. (2017) from crosswind transects inside the planetary boundary layer (PBL) of the urban plume of Manaus downwind. Considering the scenario C0, representing the emission inventory of current conditions for the region, the values found in this study stayed in the 84–207 ppb range, where the most variations in the concentration were observed in the lower vertical levels of the model,

Table 6. Evaluation indexes for model performance of meteorological variables during the simulation period (baseline scenario C0).

Variable	Station	Mean_{obs}	Mean_{sim}	σ_{obs}	σ_{sim}	r	MB	RMSE	S_{pielke}
	Colégio Militar	29.6	28.8	2.3	1.7	0.91	−0.8	1.3	1.9
Temperature (°C)	IFAM	28.2	28.5	2.8	1.8	0.88	0.3	1.5	1.6
	T1	30.0	28.5	2.5	1.8	0.88	−1.5	1.9	2.9
	T3	26.6	26.5	2.6	2.5	0.87	−0.1	1.3	1.1
	Colégio Militar	73.6	70.7	9.1	8.1	0.89	−2.9	5.1	1.7
Relative humidity (%)	IFAM	80.4	72.1	10.5	7.2	0.89	−8.3	9.7	3.7
	T1	73.9	71.8	9.3	8.2	0.88	−2.1	4.8	1.5
	T3	89.8	79.7	10.6	8.7	0.71	−10.1	12.6	3.9

Table 7. Evaluation indexes for model performance of air pollutants during the simulation period (baseline scenario C0).

Variable	Mean_{obs}	Mean_{sim}	σ_{obs}	σ_{sim}	r	MB	MNBE (%)	MNG (%)
$\text{PM}_{2.5}$ (ug m^{-3})	1.30	1.96	0.81	0.93	0.72	0.66	50.8	57.3
NO_x (ppb)	88.7	62.5	53	52.7	0.53	−26.2	−29.5	47.4
CO (ppb)	382.6	247.3	296.3	93.3	0.53	−135.3	−35.4	53.1

as expected. It is not possible to say that the model is over-predicting the actual value, since it is associated with different periods. In addition, the simulated concentrations are much lower than the CO concentrations observed in previous measurements for the dry season in Amazonas, under strong effects of biomass burning emission (e.g., Crutzen et al., 1985). O_3 mixing ratios reported by Kuhn et al. (2010) varied from 21 ppb in the adjacent background to a peak value of 63 ppb for O_3 within the PBL at 100 km distance from Manaus. In the simulated scenario C0, the peak values were in the range 26–29 ppb within the PBL and 40 ppb above it. O_3 mixing ratios downwind of Manaus under the influence of anthropogenic pollution were also reported by Trebs et al. (2012) and were on average 31 ± 14 ppb, with peak values of 60 ppb at a distance of 19 km downwind of Manaus. Such results are in good agreement with the results in this work: 10–43 ppb for the adjacent levels to 400 m at 10 km west of Manaus, considering the current conditions given by scenario C0.

In terms of previous numerical studies in the Manaus urban-influenced area, Kuhn et al. (2010) applied a single-column chemistry and meteorological model (Ganzeveld et al., 2002). Two numerical experiments were performed to assess the westward-moving plume, the first one performed by using anthropogenic emission fluxes from the EDGAR 3.2 emission database, but with the pollutant flux based on the $1° \times 1°$ grid point of the location of the city of São Paulo, increased by a factor of 7, due to the absence of a local emission inventory for Manaus. In this scenario, the simulated CO, NO_x and O_3 mixing ratios at approximately 400 m altitude and 10 km downwind were approximately 140, 4, and 50 ppb, respectively. The impact of stationary sources was evaluated in a second scenario by the inclusion of four ther-

mal power plants, adding a total of $1.5 \text{ kg NO}_x \text{ day}^{-1}$. As a result, the simulated NO_x and O_3 mixing ratios changed to 30 and 35 ppb, respectively. The significant effects of thermal power plants are also evidenced in the present study by the low concentration of NO_x in the scenarios C1 and C2 (which do not include the stationary emission sources), compared to C0 (current conditions).

3.2   Scenario emissions

The discussions on the simulation results related to scenario emissions were analyzed in the lowest model level and divided in three topics – that is, the analysis of the mean and peak behavior of pollutants, spatial analysis, and temporal evaluation described below.

3.2.1   Mean and peak behavior of pollutants

Identifying the differences between scenarios in atmosphere models with elevated complexity is not a straightforward task, due to the large number of components involved, with each of them partially contributing to the evolution of the concentrations in both time and space. In this sense, their impacts on peak average values as in the spatial average should be evaluated. For this purpose, the methodology for microphysical variable proposed by Martins et al. (2009) has been adapted to evaluate the air pollutants in this study. There are two average properties. The first is the spatial average–temporal average (SATA), which represents a mean value average both spatially and over time, and the second one is the spatial peak–temporal average (SPTA), which corresponds to the spatial peak average over time. The calculation of the values was based on 87 % of the study grid, removing five points of the grid in each extremity, which were the values
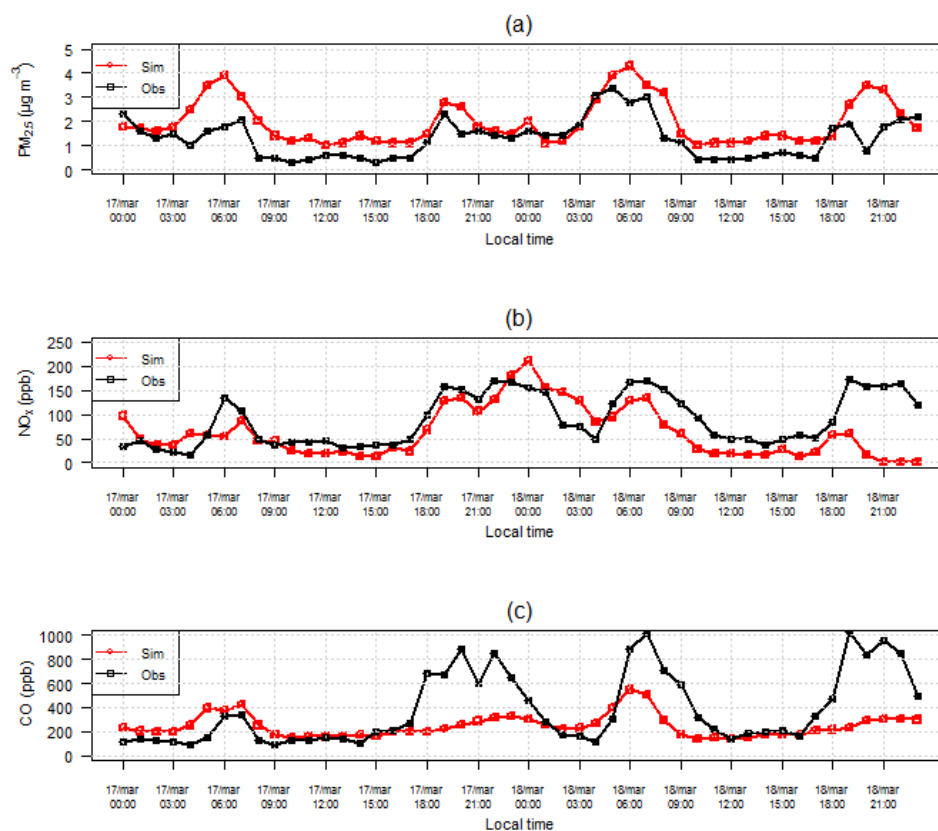
Figure 5. Temporal evaluation of simulated and observed values for the concentration of pollutants at T1: **(a)** PM$_{2.5}$, **(b)** NO$_x$ and **(c)** CO.

recommended by Skamarock et al. (2008) to reduce the effects of lateral boundary conditions. It is important to emphasize that, due to the large number of chemicals involved in the VOC, the evaluation has been conducted by summing all output model compounds.

The impact of the different scenarios evaluated according to the spatial average (SATA) and peak (SPTA) concentrations is shown in Table 8. As expected, the lower concentrations of SATA and SPTA of all pollutants are those obtained from natural conditions (scenario C1). Similarly, the future scenario (C4) has shown the highest concentrations simulated for the parameters considered. Considering the current conditions of the region (C0), scenario C4 represents an increase of approximately 35, 3, 62, 4, 16 42 and 41 % (SATA) and 45, 63, 88, 45, 109, 60 and 56 % (SPTA) for the pollutants NO$_x$, CO, SO$_2$, O$_3$, VOCs, PM$_{2.5}$ and PM$_{10}$, respectively. In terms of the individual contribution by sources, it was observed that the emission contributions from stationary sources, predominantly TPPs (scenario C3), were greater than the mobile sources (C2) for all analyzed pollutants, except for CO. For instance, the average concentration is more than double for NO$_x$ and about 1 order of magnitude greater for peak values of PM$_{10}$. This indicates that the TPPs are mainly responsible for the high concentrations of most chemical species in the grid. The influence of matrix change is dis-

cussed in the companion paper of Medeiros et al. (2017), and more details can found in this paper.

3.2.2　Spatial analysis

In order to analyze the spatial extent and location of impact of the plume of Manaus, the spatial distributions of pollutants have been evaluated. The scenario distributions have indicated that the pollution plume from Manaus could have a great impact on the surrounding area, with predominance to the west and southwest directions. The impact is both on the spatial average and spatial peak values. It has been observed that the high values of emission rates from TPPs significantly contribute to the increase in the air pollution plume area of Manaus during its spread. The influence is predominant in adjacent regions, but it can be extended over more than a hundred kilometers to the west and southwest of the city, to areas that were dominated by the original forest. As an example, Fig. 6 illustrates the spatial distributions of PM$_{2.5}$ concentration for 22:00 local time, on 18 March 2014.

For PM$_{2.5}$, considering the contour lines greater than or equal to 5 µg m^{-3}, which is the value of 10 % of the SPTA (peak value) of the future scenario, it can be observed that the largest fractions of plume covering the area as shown in Fig. 6 were 3024 km^2 (C0), 1386 km^2 (C3), and 6102 km^2

Table 8. Spatial average–temporal average (SATA) and spatial peak–temporal average (SPTA) of the concentration of trace gases and particles, in the various scenarios*.

Variable		Unit	C0	C1	C2	C3	C4
NO_x	SPTA	ppb	208.68	1.27	40.81	198.21	302.85
NO_x	SATA	ppb	1.02	0.11	0.42	0.80	1.38
CO	SPTA	ppb	291.51	83.37	261.74	174.68	476.13
CO	SATA	ppb	84.75	81.20	83.77	82.31	87.60
SO_2	SPTA	ppb	278.96	0.10	1.83	275.46	525.78
SO_2	SATA	ppb	0.85	0.06	0.08	0.79	1.38
O_3	SPTA	ppb	96.32	32.49	50.82	91.24	139.62
O_3	SATA	ppb	26.49	23.70	25.01	25.68	27.60
VOCs	SPTA	ppb	1814	35.66	77.87	1853	3799
VOCs	SATA	ppb	19.31	15.67	16.31	19.17	22.45
$PM_{2.5}$	SPTA	$\mu g\,m^{-3}$	32.51	0.35	3.49	32.38	51.89
$PM_{2.5}$	SATA	$\mu g\,m^{-3}$	0.48	0.19	0.25	0.42	0.68
PM_{10}	SPTA	$\mu g\,m^{-3}$	40.72	0.35	4.51	40.47	63.36
PM_{10}	SATA	$\mu g\,m^{-3}$	0.51	0.19	0.26	0.44	0.72

* Baseline scenario (emissions by biogenic, mobile and stationary sources); C1, only natural emissions; C2, scenario referring to natural and mobile emissions; C3, scenario representing natural and stationary emissions; C4, future scenario that includes natural emissions and doubled emissions from mobile and stationary sources.

Table 9. Area (km^2) influenced by the pollution plume, represented as a function of Manaus urban area, for all simulated scenarios.

Variable	C0	C1	C2	C3	C4
NO_x (contour lines ≥ 30 ppb) 08:00 LT – 18 Mar 2014	6	–	2	4	8
CO (contour lines ≥ 200 ppb) 08:00 LT – 18 Mar 2014	3	–	3	0.1	6
SO_2 (contour lines ≥ 50 ppb) 20:00 LT – 18 Mar 2014	1	–	–	1	2
O_3 (contour lines ≥ 50 ppb) 17:00 LT – 18 Mar 2014	20	–	3	15	26
VOCs (contour lines ≥ 100 ppb) 08:00 LT – 18 Mar 2014	6	–	–	6	11
$PM_{2.5}$ (contour lines $\geq 5\,\mu g\,m^{-3}$) 22:00 LT – 18 Mar 2014	8	–	–	4	16
PM_{10} (contour lines $\geq 5\,\mu g\,m^{-3}$) 22:00 LT – 18 Mar 2014	8	–	0.1	4	17

(C4). Based on the plume covering the area and on the contour lines established, for the future scenario, an area 16-fold greater than the Manaus urban area (MUA) has been observed, which is approximately 377 km^2. In addition, there were no concentrations on the simulation by vehicular sources (C2) within the established contour. The values of the influence in an area and their contour lines for other pollutants are summarized in Table 9 as a function of MUA.

3.2.3 Temporal evaluation

Considering the importance of assessing the temporal development of the concentrations for a locality, two distinct points have been selected. The first one was located within the city of Manaus near the T1 station, and the second in a predominant direction of the plume propagation at approximately 84 km southwest (T3), which can be identified in Fig. 1. It is important to emphasize that the points were chosen in accordance with the highest concentrations of special distribution observed. From this evaluation, the important role of the stationary sources in the results of the concentrations of air pollutants has become evident. For example, based on Fig. 7, the highest NO_x concentrations are found in scenario C4, followed by C0 and C3, following the trends presented by SATA and SPTA. Even in locations that are distant from the city of Manaus, high concentrations when compared to concentrations in conditions not influenced by human activities (scenario C1) have been covered. In addi-
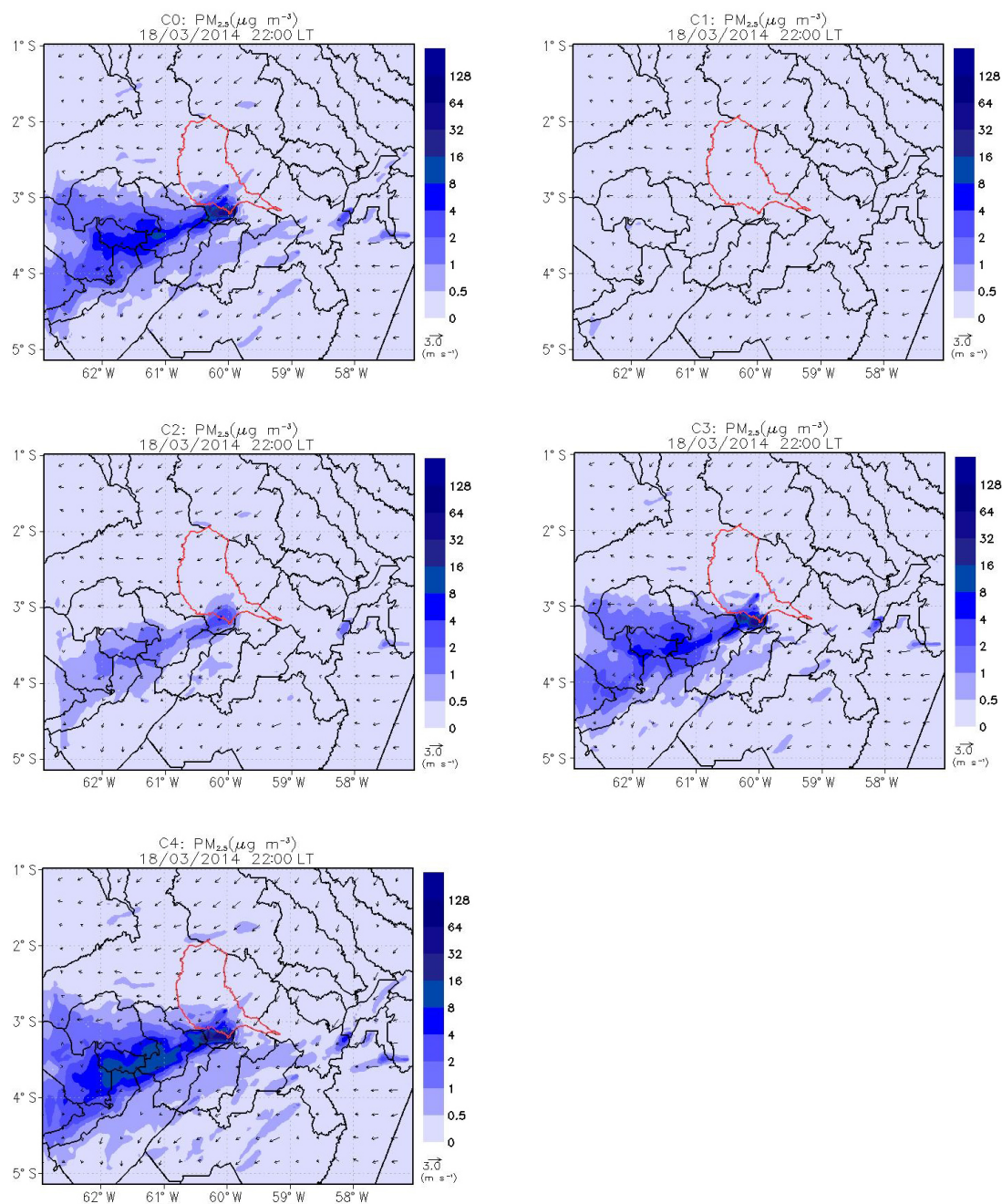
Figure 6. Spatial distribution of the scenarios studied for PM$_{2.5}$ concentration, calculated at 22:00, local time, on 18 March 2014. The black contours illustrate the delimitations of the municipalities on the grid, and the red one represents Manaus.

tion, it has been observed that all scenarios with the participation of TPPs have a significant impact on the direction of the plume spread, while scenarios C1 and C2 remained with their concentrations near zero. This observation reinforces the fact that the purely vehicular source plume could not produce significant impact over long distances.

4 Discussions and conclusions

The main purpose of this study was to represent the daily cycle of anthropogenic and biogenic emissions that are not available in global inventories which promote the development of air pollution plumes in the city of Manaus. In this sense, to support new design of regulations, it is important to investigate the relative contribution of the mobile and stationary sources as well the area impacted by urban pollu-
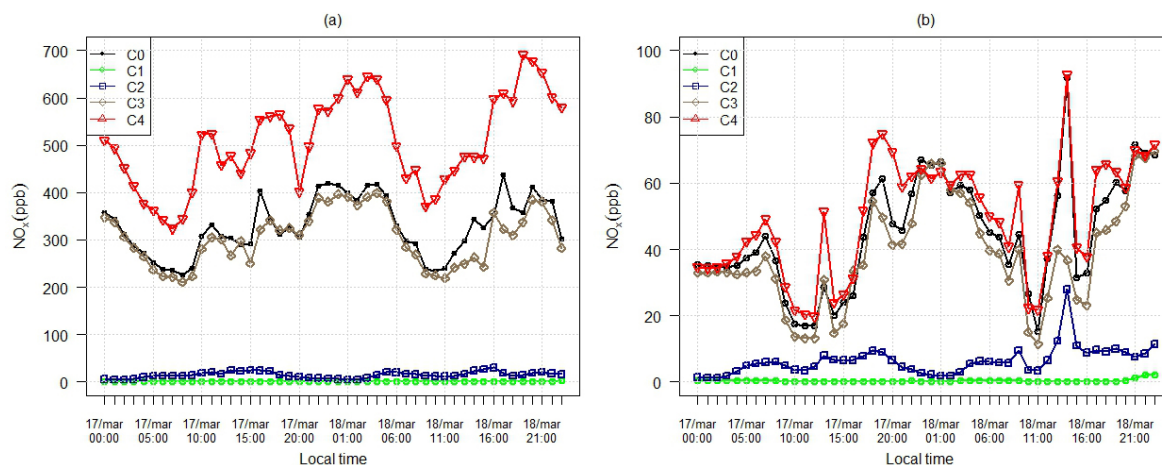
Figure 7. Temporal evaluation of NO_x. Panel **(a)** represents the concentration within Manaus, while panel **(b)** refers to the point towards the pollution plume about 84 km southwest.

tion plume. However, the conclusions presented here should be viewed with caution since the simulations involve only two specific days and they are not representative of the entire year.

According to the statistical criteria used for the type of model considered, comparing the observed data with the simulation results to the current state of emissions defined by the baseline scenario (C0), we concluded that the WRF-Chem performance can be considered satisfactory due to the representative criteria for most meteorological fields and air pollutants.

Based on the analyses of observed average and peak concentrations of pollutants, as well as the spatial and temporal distribution of numerical studies, it is clear that stationary sources have an important role in the contribution of human activity in Manaus. The exception is given for carbon monoxide, which has shown few significant contributions. For a comparative evaluation of the results presented herein and those in the literature, it has been observed that there is no parallelism with studies of other parts of the world that have an urban area in a vast tropical forest cover. Several studies have been identified in which the contribution of thermal power plants is higher than the vehicle sources, presenting preserved natural environment conditions, as occurs in Manaus. Studies such as Reddy and Venkataramn (2002) from India show that the main emission of a particulate matter and sulfur dioxide originates from fossil fuel power plants. In this example, SO_2 emissions by power plants are responsible for over 60 % of the country's emissions. In another example, in a study performed in China, Zhang et al. (2012) conclude that most $PM_{2.5}$ (nitrate and sulfate) sources are from the energy sector, mainly power plants, exceeding the combined contribution of industrial, residential and transport sources. Also from China, results by Huang et al. (2011) estimate that stationary sources contribute in approximately 97, 86, 89, 91

and 69 % of the total emissions of SO_2, NO_x, PM_{10}, $PM_{2.5}$ and VOC, respectively.

In the specific case of Manaus, it is important to emphasize that the only hydroelectric plant located in the region that is able to bring electricity to Manaus is the Balbina hydroelectric power station. It has an average capacity of only 250 MW and it contributes to less than 15 % of the electricity used in Manaus (ANEEL, 2014). Therefore, the largest source of electricity for the region comes from power plants burning petroleum fuels, particularly fuel oil and diesel, with higher emission factors if compared, for example, to natural gas.

Another relevant issue is the high electricity consumption of Manaus. According to data from the Brazilian Energy Research Company (EPE) (www.epe.gov.br/), the electricity consumption per capita in Brazil is 2.5 MWh per year, whereas in the city of Manaus the consumption is 7.2 MWh, about 3 times higher. Two aspects make the region highly dependent on electricity. The first is the incentive policies for the consolidation of the industrial area in Manaus in order to foster the economic development of the region. This resulted in a region with a variety of industrial centers, with a high demand for electricity. The second aspect is the fact that the city is located in a humid equatorial climate region, dominated by high temperatures and humidity, as well as little ventilation and torrential rains throughout the year. Such environmental characteristics induce high electricity consumption by both residential and commercial sectors, resulting in the greater burning of fossil fuel power plants that intensify the concentrations of air pollutants.

The spatial distributions of these scenarios indicated that the pollution plume from Manaus could have a great impact on the surrounding areas, mainly in west and southwest directions, reaching hundreds of kilometers from the city. Since most thermal power plants and the REMAN refinery are lo-

cated near the banks of the Negro and Solimões rivers, the plume transportation could be influenced by the circulation of river breezes, which defines the trajectory of pollutants. Although the breeze effect is not focused on this paper, this evaluation has been confirmed by other studies for the large rivers in the Amazon, for instance Santos et al. (2014).

Finally, in order to evaluate the potential urban growth in that region, a future scenario has been designed. In summary, this scenario has shown the impact of a possible increase in mobile and stationary emissions in the study region, including the expansion of the urban area. The approach of future scenarios has been studied using several methodologies, mainly in Asia (Zhou et al., 2003; Ohara et al., 2007). In all cases, the increase in air pollution concentrations (e.g., 2020 scenario showed an increase of 12 % in CO concentration) could be observed if the current conditions of the energy matrix were maintained. However, there is the possibility of reductions and a decrease in emission rates by using sustainable energies.

The Supplement related to this article is available online at https://doi.org/10.5194/acp-17-7977-2017-supplement.

References

Ackermann, I. J., Hass, H., Memmesheimer, M., Ebel, A., Binkowski, F. A., and Shankar, U.: Modal aerosol dynamics model for Europe: Development and first applications, Atmos. Environ., 32, 2981–2999, 1998.

Albuquerque, T. T. A., Andrade, M. F., and Ynoue, R. Y.: Characterization of atmospheric aerosols in the city of Sao Paulo, Brazil: comparisons between polluted and unpolluted periods, Water Air Soil Poll., 195, 201–213, 2011.

Alves, E. G., Jardine, K., Tota, J., Jardine, A., Yãnez-Serrano, A. M., Karl, T., Tavares, J., Nelson, B., Gu, D., Stavrakou, T., Martin, S., Artaxo, P., Manzi, A., and Guenther, A.: Seasonality of isoprenoid emissions from a primary rainforest in central Amazonia, Atmos. Chem. Phys., 16, 3903–3925, https://doi.org/10.5194/acp-16-3903-2016, 2016.

Andrade, M. F., Ynoe, R. Y., Freitas, E. D., Todesco, E., Vela, A. V., Ibarra, S., Martins, L. D., Martins, J. A., and Carvalho, V. S. B.: Air quality forecasting system for southeastern Brazil, Front. Environ. Sci., 3, https://doi.org/10.3389/fenvs.2015.00009, 2015.

Andreae, M. O. and Merlet, P.: Emission of trace gases and aerosols from biomass burning, Global Biogeochem. Cy., 15, 955–966, 2001.

Andreae, M. O., Artaxo, P., Beck, V., Bela, M., Freitas, S., Gerbig, C., Longo, K., Munger, J. W., Wiedemann, K. T., and Wofsy, S. C.: Carbon monoxide and related trace gases and aerosols over the Amazon Basin during the wet and dry seasons, Atmos. Chem. Phys., 12, 6041–6065, https://doi.org/10.5194/acp-12-6041-2012, 2012.

ANEEL: Agência Nacional de Energia Elétrica. Banco de Informações de Geração: BIG, available at: http://www.aneel.gov.br/aplicacoes/capacidadebrasil/GeracaoTipoFase.asp?tipo=2andfase=3 (last access: August 2014), 2014.

ANP: Agência Nacional de Petróleo. Vendas pelas distribuidoras dos derivados dos combustíveis de petróleo, available at: http://www.anp.gov.br/ (last access: January 2015), 2014a.

ANP: Agência Nacional de Petróleo Volume de Petróleo refinado por refinaria, available at: http://www.anp.gov.br/preco (last access: January 2015), 2014b.

Araújo, A. C., Nobre, A. D., Kruijt, B., Elbers, J. A., Dallarosa, R., Stefani, P., von Randow, C., Manzi, A. O., Culf, A. D., Gash, J. H. C., Valentini, R., and Kabat, P.: Comparative measurements of carbon dioxide fluxes from two nearby towers in a central Amazonian rainforest: The Manaus LBA site, J. Geophys. Res., 107, 8090, https://doi.org/10.1029/2001JD000676, 2002.

Artaxo, P., Rizzo, L. V., Brito, J. F., Barbosa, H. M. J., Arana, A., Sena, E. T., Cirino, G. G., Bastos, W., Martin, S. T., and Andreae, M. O.: Atmospheric aerosols in Amazonia and land use change: from natural biogenic to biomass burning conditions, Faraday Discuss., 165, 203–235, 2013.

Atkinson, R.: Atmospheric chemistry of VOCs and NO$_x$, Atmos. Environ., 34, 2063–2101 https://doi.org/10.1016/S1352-2310(99)00460-4, 2000.

Baars, H., Ansmann, A., Althausen, D., Engelmann, R., Heese, B., Muller, D., Artaxo, P., Paixao, M., Pauliquevis, T., and Souza, R.: Aerosol profiling with lidar in the Amazon Basin during the wet and dry season, J. Geophys. Res., 117, https://doi.org/10.1029/2012JD018338, 2012.

Bateman, A. P., Gong, Z., Harder, T. H., de Sá, S. S., Wang, B., Castillo, P., China, S., Liu, Y., O'Brien, R. E., Palm, B. B., Shiu, H.-W., Cirino, G. G., Thalman, R., Adachi, K., Alexander, M. L., Artaxo, P., Bertram, A. K., Buseck, P. R., Gilles, M. K., Jimenez, J. L., Laskin, A., Manzi, A. O., Sedlacek, A., Souza, R. A. F., Wang, J., Zaveri, R., and Martin, S. T.: Anthropogenic influences on the physical state of submicron particulate mat-

ter over a tropical forest, Atmos. Chem. Phys., 17, 1759–1773, https://doi.org/10.5194/acp-17-1759-2017, 2017.

Beck, V., Gerbig, C., Koch, T., Bela, M. M., Longo, K. M., Freitas, S. R., Kaplan, J. O., Prigent, C., Bergamaschi, P., and Heimann, M.: WRF-Chem simulations in the Amazon region during wet and dry season transitions: evaluation of methane models and wetland inundation maps, Atmos. Chem. Phys., 13, 7961–7982, https://doi.org/10.5194/acp-13-7961-2013, 2013.

Bela, M. M., Longo, K. M., Freitas, S. R., Moreira, D. S., Beck, V., Wofsy, S. C., Gerbig, C., Wiedemann, K., Andreae, M. O., and Artaxo, P.: Ozone production and transport over the Amazon Basin during the dry-to-wet and wet-to-dry transition seasons, Atmos. Chem. Phys., 15, 757–782, https://doi.org/10.5194/acp-15-757-2015, 2015.

Binkowski, F. S. and Skankar, U.: The regional particulate matter model, mode description and preliminary results, J. Geophys. Res., 100, 26191–26209, 1995.

Brito, J., Rizzo, L. V., Herckes, P., Vasconcellos, P. C., Caumo, S. E. S., Fornaro, A., Ynoue, R. Y., Artaxo, P., and Andrade, M. F.: Physical–chemical characterisation of the particulate matter inside two road tunnels in the São Paulo Metropolitan Area, Atmos. Chem. Phys., 13, 12199–12213, https://doi.org/10.5194/acp-13-12199-2013, 2013.

Capucim, M. N., Brand, V. S., Machado, C. B., Martins, L. D., Allasia, D. G., Homann, C. T., Freitas, E. D., Silva Dias, M. F. A., Martins, J. A.: South America Land Use and Land Cover Assessment and Preliminary Analysis of Their Impacts on Regional Atmospheric Modeling Studies, IEEE J. Sel. Top. Appl., 8, 1185–1198, 2015.

Carvalho, V. S. B., Freitas, E. D., Martins, L. D., Martins, J. A., Mazzoli, C. R., and Andrade, M. d. F.: Air quality status and trends over the Metropolitan Area of São Paulo, Brazil as a result of emission control policies, Environ. Sci. Policy, 47, 68–79, 2015.

Cecchini, M. A., Machado, L. A. T., Comstock, J. M., Mei, F., Wang, J., Fan, J., Tomlinson, J. M., Schmid, B., Albrecht, R., Martin, S. T., and Artaxo, P.: Impacts of the Manaus pollution plume on the microphysical properties of Amazonian warmphase clouds in the wet season, Atmos. Chem. Phys., 16, 7029–7041, https://doi.org/10.5194/acp-16-7029-2016, 2016.

CETESB: Companhia Ambiental do Estado de São Paulo. Inventário de emissões das fontes estacionárias do estado de São Paulo, 2009.

Chang, J. S., Binkowski, F. S., Seaman, N. L., Mchenry, J. N., Samson, P. J., Stockwell, W. R., Walcek, C. J., Madronich, S., Middleton, P. B., Pleim, J. E., and Lansford, H. H.: The regional acid deposition model and engineering model, State-of-Science/Technology, Report 4, National Acid Precipitation Assessment Program, Washington, DC, 1989.

Chen, F. and Dudhia, J.: Coupling an advanced land surface–hydrology model with the Penn State – NCAR MM5 modeling system. Part I: Model implementation and sensitivity, Mon. Weather Rev., 129, 569–585, 2001.

Crompton, P. and Wu, Y.: Energy consumption in China: past trends and future directions, Energy Econ., 27, 195–208, 2005.

Crutzen, P. J., Delany, A. C., Greenberg, J., Haagenson, P., Heidt, L., Lueb, R., Pollock, W., Seiler, W., Wartburg, A., and Zimmerman, P.: Tropospheric chemical-composition measurements in Brazil during the dry season, J. Atmos. Chem., 2, 233–256, 1985.

DENATRAN: Departamento Nacional de Trânsito Frota de veículos por tipos de combustível e município, available at: http://www.denatran.gov.br, last access: March 2014.

de Sá, S. S., Palm, B. B., Campuzano-Jost, P., Day, D. A., Newburn, M. K., Hu, W., Isaacman-VanWertz, G., Yee, L. D., Thalman, R., Brito, J., Carbone, S., Artaxo, P., Goldstein, A. H., Manzi, A. O., Souza, R. A. F., Mei, F., Shilling, J. E., Springston, S. R., Wang, J., Surratt, J. D., Alexander, M. L., Jimenez, J. L., and Martin, S. T.: Influence of urban pollution on the production of organic particulate matter from isoprene epoxydiols in central Amazonia, Atmos. Chem. Phys., 17, 6611–6629, https://doi.org/10.5194/acp-17-6611-2017, 2017.

Dudhia, J.: Numerical study of convection observed during the winter monsoon experiment using a mesoscale two-dimensional model, J. Atmos. Sci, 46, 3077–3107, 1989.

ELETROBRAS: Plano anual de operação dos sistemas isolados para 2014, 2013.

EPA: Environmental Protection Agency. Air emissions species manual, volume I: voltaic organic compound species profiles, Research Triangle Park, 698 pp., 1990.

EPA: Environmental Protection Agency. Complilation of air pollutant emission factors, volume 1: Stationary point and are sources, 5th Edn., AP-42. Research Triangle Park, North Carolina, 697 pp., 1998.

EPA: Environmental Protection Agency. Air Pollutant Emission Inventory Guidebook 2009, 2010.

Fisch, G., Marengo, J. A., and Nobre, C. A.: Uma revisão geral sobre o clima da Amazônia, Acta Amazonica, 28, 101–126, 1998.

Freitas, S. R., Longo, K. M., and Andreae, M. O.: Impact of including the plume rise of vegetation fires in numerical simulations of associated atmospheric pollutants, Geophys. Res. Lett., 33, L17808, https://doi.org/10.1029/2006GL026608, 2006.

Ganzeveld, L. N., Lelieveld, J., Dentener, F. J., Krol, M. C., and Roelofs, G. J.: Atmosphere-biosphere trace gas exchanges simulated with a single-column model, J. Geophys. Res.-Atmos., 107, 4297, https://doi.org/10.1029/2001JD000684, 2002.

Grell, G., Peckham, S., Schmitz, R., Mckeen, S., Frost, G., Skamarock, W., and Eder, B.: Fully coupled "online" chemistry within the WRF model, Atmos. Environ., 39, 6957–6976, 2005.

Guenther, A. B., Zimmerman, P. R., Harley, P. C., Monson, R. K., and Fall, R.: Isoprene and monoterpene emission rate variability: Model evaluations and sensitivity analyses, J. Geophys. Res., 98D, 12609–12617, 1993.

Guenther, A., Zimmerman, P., and Wildermuth, M.: Natural volatile organic compound emission rate estimates for U.S. Woodland landscapes, Atmos. Environ., 28, 1197–1210, 1994.

Guo, H., Jiang, F., Cheng, H. R., Simpson, I. J., Wang, X. M., Ding, A. J., Wang, T. J., Saunders, S. M., Wang, T., Lam, S. H. M., Blake, D. R., Zhang, Y. L., and Xie, M.: Concurrent observations of air pollutants at two sites in the Pearl River Delta and the implication of regional transport, Atmos. Chem. Phys., 9, 7343–7360, https://doi.org/10.5194/acp-9-7343-2009, 2009.

Hallak, R. and Perreira Filho, A. J.: Metodologia para análise de desempenho de simulações de sistemas convectivos na região metropolitana de São Paulo com o modelo ARPS: sensibilidade a variações com os esquemas de advecção e assimilação de dados, Revista Brasileira de Meteorologia, 26, 591–608, 2011.

Han, K. M., Song, C. H., Ahn, H. J., Park, R. S., Woo, J. H., Lee, C. K., Richter, A., Burrows, J. P., Kim, J. Y., and Hong, J. H.: In-

vestigation of NO_x emissions and NO_x-related chemistry in East Asia using CMAQ-predicted and GOME-derived NO_2 columns, Atmos. Chem. Phys., 9, 1017–1036, https://doi.org/10.5194/acp-9-1017-2009, 2009.

Hong, S. Y. and Dudhia, J.: Testing of a new non-local boundary layer vertical diffusion scheme in numerical weather prediction applications, in: 20th Conference on Weather Analysis and Forecasting/16th Conference on Numerical Weather Prediction, Seattle, WA, 2003.

Hu, W., Palm, B. B., Day, D. A., Campuzano-Jost, P., Krechmer, J. E., Peng, Z., de Sá, S. S., Martin, S. T., Alexander, M. L., Baumann, K., Hacker, L., Kiendler-Scharr, A., Koss, A. R., de Gouw, J. A., Goldstein, A. H., Seco, R., Sjostedt, S. J., Park, J.-H., Guenther, A. B., Kim, S., Canonaco, F., Prévôt, A. S. H., Brune, W. H., and Jimenez, J. L.: Volatility and lifetime against OH heterogeneous reaction of ambient isoprene-epoxydiols-derived secondary organic aerosol (IEPOX-SOA), Atmos. Chem. Phys., 16, 11563–11580, https://doi.org/10.5194/acp-16-11563-2016, 2016.

Hu, X.-M., Fuentes, J. D., and Zhang, F.: Downward transport and modification of tropospheric ozone through moist convection, J. Atmos. Chem., 65, 13–35, https://doi.org/10.1007/s10874-010-9179-5, 2010.

Huang, C., Chen, C. H., Li, L., Cheng, Z., Wang, H. L., Huang, H. Y., Streets, D. G., Wang, Y. J., Zhang, G. F., and Chen, Y. R.: Emission inventory of anthropogenic air pollutants and VOC species in the Yangtze River Delta region, China, Atmos. Chem. Phys., 11, 4105–4120, https://doi.org/10.5194/acp-11-4105-2011, 2011.

IBGE: Instituto Brasileiro de Geografia e Estatística. Censo Demográfico, available at: http://cidades.ibge.gov.br/xtras/perfil.php?codmun=_130260 last access: August 2014.

Jardine, K. J., Jardine, A. B., Souza, V. F., Carneiro, V., Ceron, J. V., Gimenez, B. O., Soares, C. P., Durgante, F. M., Higuchi, N., Manzi, A. O., Gonccalves, J. F. C., Garcia, S., Martin, S. T., Zorzanelli, R. F., Piva, L. R., and Chambers, J. Q.: Methanol and isoprene emissions from the fast growing tropical pioneer species Vismia guianensis (Aubl.) Pers. (Hypericaceae) in the central Amazon forest, Atmos. Chem. Phys., 16, 6441–6452, https://doi.org/10.5194/acp-16-6441-2016, 2016.

Jiang, F., Liu, Q., Huang, X., Wang, T., Zhuang, B., and Xie, M.: Regional modeling of secondary organic aerosol over China using WRF/Chem, J. Aerosol Sci., 43, 57–73, 2012.

Kampa, M. and Castanas, E.: Human health effects of air pollution, Environ. Pollut., 151, 362–367, 2008.

Kourtchev, I., Godoi, R. H. M., Connors, S., Levine, J. G., Archibald, A. T., Godoi, A. F. L., Paralovo, S. L., Barbosa, C. G. G., Souza, R. A. F., Manzi, A. O., Seco, R., Sjostedt, S., Park, J.-H., Guenther, A., Kim, S., Smith, J., Martin, S. T., and Kalberer, M.: Molecular composition of organic aerosols in central Amazonia: an ultra-high-resolution mass spectrometry study, Atmos. Chem. Phys., 16, 11899–11913, https://doi.org/10.5194/acp-16-11899-2016, 2016.

Kuhn, U., Ganzeveld, L., Thielmann, A., Dindorf, T., Schebeske, G., Welling, M., Sciare, J., Roberts, G., Meixner, F. X., Kesselmeier, J., Lelieveld, J., Kolle, O., Ciccioli, P., Lloyd, J., Trentmann, J., Artaxo, P., and Andreae, M. O.: Impact of Manaus City on the Amazon Green Ocean atmosphere: ozone production,

precursor sensitivity and aerosol load, Atmos. Chem. Phys., 10, 9251–9282, https://doi.org/10.5194/acp-10-9251-2010, 2010.

Kuik, F., Lauer, A., Beukes, J. P., Van Zyl, P. G., Josipovic, M., Vakkari, V., Laakso, L., and Feig, G. T.: The anthropogenic contribution to atmospheric black carbon concentrations in southern Africa: a WRF-Chem modeling study, Atmos. Chem. Phys., 15, 8809–8830, https://doi.org/10.5194/acp-15-8809-2015, 2015.

Lin, M., Holloway, T., Carmichael, G. R., and Fiore, A. M.: Quantifying pollution inflow and outflow over East Asia in spring with regional and global models, Atmos. Chem. Phys., 10, 4221–4239, https://doi.org/10.5194/acp-10-4221-2010, 2010.

Liu, S. C., McKeen, S. A., Hsie, E. Y., Lin, X., Kelly, K. K., Bradshaw, J. D., Sandholm, S. T., Browell, E. V., Gregory, G. L., Sachse, G. W., Bandy, A. R., Thornton, D. C., Blake, D. R., Rowland, F. S., Newell, R., Heikes, B. G., Singh, H., and Talbot, R. W.: Model study of tropospheric trace species distributions during PEM-West A, J. Geophys. Res., 101, 2073–2085, 1996.

Lowe, D., Archer-Nicholls, S., Morgan, W., Allan, J., Utembe, S., Ouyang, B., Aruffo, E., Le Breton, M., Zaveri, R. A., Di Carlo, P., Percival, C., Coe, H., Jones, R., and McFiggans, G.: WRF-Chem model predictions of the regional impacts of N_2O_5 heterogeneous processes on night-time chemistry over north-western Europe, Atmos. Chem. Phys., 15, 1385–1409, https://doi.org/10.5194/acp-15-1385-2015, 2015.

Lutz, W., Sanderson, W., and Scherbov, S.: The end of world population growth. Nature, 412, 543–545, 2001.

MACCity emissions dataset: available at: http://eccad.sedoo.fr/eccad_extract_interface/JSF/page_species.jsf (last access: May 2017), 2014.

MANAUS: Projeto Geo Cidades. Relatório ambiental urbano integrado: informe GEO, Manaus/Supervisão, 2002.

Martins, J. A. and Silva Dias, M. A. F.: The impact of smoke from forest fires on the spectral dispersion of cloud droplet size distributions in the Amazonian region, Environ. Res. Lett., 4, 015002, https://doi.org/10.1088/1748-9326/4/1/015002, 2009.

Martins, J. A., Martins, L. D., Freitas, E. D., Mazzoli, C. R., Hallak, R., and Andrade, M. F.: Aplicação de imagens de satélite no desenvolvimento de inventários de emissão de alta resolução, Congresso Brasileiro de Meteorologia, São Paulo, 2008.

Martins, J. A., Silva Dias, M. A. F., and Goncalves, F. L. T.: Impact of biomass burning aerosols on precipitation in the Amazon: a modelling case study, J. Geophys. Res., 114, D02207, https://doi.org/10.1029/2007JD009587, 2009.

Martin, S. T., Artaxo, P., Machado, L. A. T., Manzi, A. O., Souza, R. A. F., Schumacher, C., Wang, J., Andreae, M. O., Barbosa, H. M. J., Fan, J., Fisch, G., Goldstein, A. H., Guenther, A., Jimenez, J. L., Pöschl, U., Silva Dias, M. A., Smith, J. N., and Wendisch, M.: Introduction: Observations and Modeling of the Green Ocean Amazon (GoAmazon2014/5), Atmos. Chem. Phys., 16, 4785-4797, https://doi.org/10.5194/acp-16-4785-2016, 2016.

Martin, S. T., Artaxo, P., Machado, L., Manzi, A., Souza, R., Schumacher, C., Wang, J., Biscaro, T., Brito, J., Calheiros, A., Jardine, K., Medeiros, A., Portela, B., de Sá, S., Adachi, K., Aiken, A., Albrecht, R., Alexander, L., Andreae, M., Barbosa, H., Buseck, P., Chand, D., Comstock, J., Day, D., Dubey, M., Fan, J., Fast, J., Fisch, G., Fortner, E., Giangrande, S., Gilles, M., Goldstein, A., Guenther, A., Hubbe, J., Jensen, M., Jimenez, J., Keutsch, F., Kim, S., Kuang, C., Laskin, A., McKinney, K., Mei, F., Miller, M., Nascimento, R., Pauliquevis, T., Pekour, M., Peres, J., Petäjä,

T., Pöhlker, C., Pöschl, U., Rizzo, L., Schmid, B., Shilling, J., Dias, M., Smith, J., Tomlinson, J., Tóta, J., and Wendisch, M.: The Green Ocean Amazon Experiment (GoAmazon2014/5) Observes Pollution Affecting Gases, Aerosols, Clouds, and Rainfall over the Rain Forest, B. Am. Meteorol. Soc., 98, 981–997, https://doi.org/10.1175/BAMS-D-15-00221.1, 2017.

Martins, L. D. and Andrade, M. F.: Ozone Formation Potentials of Volatile Organic Compounds and Ozone Sensitivity to Their Emission in the Megacity of São Paulo, Brazil, Water Air Soil Pollut., 195, 201–213, https://doi.org/10.1007/s11270-008-9740-x, 2008.

Martins, L. D., Andrade, M. F., Freitas, E. D., Pretto, A., Gatti, L. V., Albuquerque, E. L., Tomaz, E., Guardani, M. L., Martins, M., and Junior, O. M. A.: Emission factors for gas-powered vehicles travelling through road tunnels in Sao Paulo, Brazil, Environ. Sci. Technol., 40, 6722–6729, 2006.

Martins, L. D., Martins, J. A., Freitas, E. D., Mazzaroli, C. R., Gonçalves, L. T., Ynoue, R. Y., Hallak, R., Albuquerque, T. T. A., and de Fatima Andrade, M.: Potential health impact of ultrafine particles under clean and polluted urban atmospheric conditions: A model-based study, Air Qual. Atmos. Health, 3, 29–39, 2010.

Medeiros, A. S. S., Calderaro, G., Guimarães, P. C., Magalhaes, M. R., Morais, M. V. B., Rafee, S. A. A., Ribeiro, I. O., Andreoli, R. V., Martins, J. A., Martins, L. D., Martin, S. T., and Souza, R. A. F.: Power Plant Fuel Switching and Air Quality in a Tropical Forested Environment, Atmos. Chem. Phys. Discuss., https://doi.org/10.5194/acp-2016-1113, in review, 2017.

Michael, M., Yadav, A., Tripathi, S. N., Kanawade, V. P., Gaur, A., Sadavarte, P., and Venkataraman, C.: Simulation of trace gases and aerosols over the Indian domain: evaluation of the WRF-Chem Model, Atmos. Chem. Phys. Discuss., 13, 12287–12336, https://doi.org/10.5194/acpd-13-12287-2013, 2013.

Milbrandt, J. A. and Yau, M. K.: A multimoment bulk microphysics parameterization. Part I: Analysis of the role of the spectral shape parameter, J. Atmos. Sci., 62, 3051–3064, 2005.

Miranda, R. M. and Andrade, M. F.: Physicochemical characteristics of atmospheric aerosol 10 during winter in the Sao Paulo metropolitan area in Brazil, Atmos. Environ., 39, 6188–6193, 2005.

Mlawer, E. J., Taubman S. J., Brown, P. D., Iacono, M. J., and Clough, S. A.: Radiative transfer for inhomogeneous atmosphere: RRTM, a validated correlated-k model for the longwave, J. Geophys. Res., 102, 16663–16682, 1997.

MMA: Ministério do Meio Ambiente. Primeiro inventário nacional de emissões atmosféricas por veículos automotores rodoviários, 2011.

Ohara, T., Akimoto, H., Kurokawa, J., Horii, N., Yamaji, K., Yan, X., and Hayasaka, T.: An Asian emission inventory of anthropogenic emission sources for the period 1980–2020, Atmos. Chem. Phys., 7, 4419–4444, https://doi.org/10.5194/acp-7-4419-2007, 2007.

Pielke, R. A.: Mesoscale meteorological modeling, 2nd Edn., International Geophysics Series, 78, 676, 2002.

Pöhlker, M. L., Pöhlker, C., Ditas, F., Klimach, T., Hrabe de Angelis, I., Araújo, A., Brito, J., Carbone, S., Cheng, Y., Chi, X., Ditz, R., Gunthe, S. S., Kesselmeier, J., Könemann, T., Lavric, J. V., Martin, S. T., Mikhailov, E., Moran-Zuloaga, D., Rose, D., Saturno, J., Su, H., Thalman, R., Walter, D., Wang, J., Wolff, S., Bar-

bosa, H. M. J., Artaxo, P., Andreae, M. O., and Pöschl, U.: Long-term observations of cloud condensation nuclei in the Amazon rain forest – Part 1: Aerosol size distribution, hygroscopicity, and new model parametrizations for CCN prediction, Atmos. Chem. Phys., 16, 15709–15740, https://doi.org/10.5194/acp-16-15709-2016, 2016.

Rafee, S. A. A., Kawashima, A. B., Morais, M. V. B., Urbina, V., Martins, L. D., and Martins, J. A.: Assessing the Impact of Using Different Land Cover Classification in Regional Modeling Studies for the Manaus Area, Brazil, Journal of Geoscience and Environment Protection, 3, 77–78, 2015.

Reddy, S. M. and Venkataraman, C.: Inventory of aerosol and sulphur dioxide emissions from India: Part I – fossil fuel combustion, Atmos. Environ., 36, 677–697, 2002.

Sánchez-Ccoyllo, O. R., Ynoue, R. Y., Martins, L. D., Astolfo, R., Miranda, R. M., Freitas, E. D., Borges, A. S., Fornaro, A., Freitas, H., Moreira, A., and Andrade, M. F.: Vehicular particulate matter emissions in road tunnels in São Paulo, Brazil, Environ. Monit. Assess., 149, 241–249, https://doi.org/10.1007/s10661-008-0198-5, 2009.

Santos, M. J., Silva Dias, M. A. F., and Freitas, D.: Influence of Local Circulations on Wind, Moisture and Precipitation Close to Manaus City, Amazon Region – Brazil, J. Geophys. Res., 119, 233–249, 2014.

Schell, B., Ackermann, I. J., Hass, H., Binkowski, F. S., and Ebel, A.: Modelling the formation of secondary organic aerosol within a comprehensive air quality model system, J. Geophys. Res., 106, 28275–28293, 2001.

Schneider, A., Friedl, M. A., and Potere, D.: A new map of global urban extent from MODIS data, Environ. Res. Lett., 4, 004003, 2009.

Schoenemeyer, T., Richter, K., and Smiatek, G.: Vorstudie uber ein raumlich und zeitlich aufgelostes Kataster anthropogener und biogener Emissionen fuer Bayern mit Entwicklung eines Prototyps und Anwendung fur Immissionsprognosen, Abschluss bericht an das Bayerische Landesamt fur Umweltschutz. Fraunhofer-Institut fuer Atmosphaerische Umweltforschung, Garmisch-Partenkirchen, 1997.

Simpson, D., Guenther, A., Hewitt, C. N., and Steinbrecher, R.: Biogenic emissions in Europe, estimates and uncertainties, J. Geophys. Res., 100D, 22875–22890, 1995.

Skamarock, W. C., Klemp, J. B., Dudhia, J., Gill, D. O., Barker, D. M., Wang, W., and Powers, J. G.: A description of the Advanced Research WRF Version 3. NCAR Tech. Note NCAR/TN-4681STR, 88 pp., 2008.

Stockwell, W. R., Middleton, P., Chang, J. S., and Tang, X.: The second-generation regional acid deposition model chemical mechanism for regional air quality modeling, J. Geophys. Res., 95, 16343–16367, 1990.

Tie, X., Madronich, S., Li, G. H., Ying, Z. M., Zhang, R., Garcia, A., Lee-Taylor, J., and Liu, Y.: Characterizations of chemical oxidants in Mexico City: a regional chemical/dynamical model (WRF-Chem) study, Atmos. Environ., 41, 1989–2008, 2007.

Tie, X., Brasseur, G., and Ying, Z.: Impact of model resolution on chemical ozone formation in Mexico City: application of the WRF-Chem model, Atmos. Chem. Phys., 10, 8983–8995, https://doi.org/10.5194/acp-10-8983-2010, 2010.

Trebs, I., Mayol-Bracero, O. L., Pauliquevis, T., Kuhn, U., Sander, R., Ganzeveld, L., Meixner, F. X., Kesselmeier, J.,

Artaxo, P., and Andreae, M. O.: Impact of the Manaus urban plume on trace gas mixing ratios near the surface in the Amazon Basin: implications for the $NONO_2$_O_3 photostationary state and peroxy radical levels, J. Geophys. Res., 117, https://doi.org/10.1029/2011JD016386, 2012.

Tuccella, P., Curci, G., Visconti, G., Bessagnet, B., Menut, L., and Park, R. J.: Modeling of gas and aerosol with WRF/Chem over Europe: evaluation and sensitivity study, J. Geophys. Res., 117, D03303, https://doi.org/10.1029/2011JD016302, 2012.

Vara-Vela, A., Andrade, M. F., Kumar, P., Ynoue, R. Y., and Muñoz, A. G.: Impact of vehicular emissions on the formation of fine particles in the Sao Paulo Metropolitan Area: a numerical study with the WRF-Chem model, Atmos. Chem. Phys., 16, 777–797, https://doi.org/10.5194/acp-16-777-2016, 2016.

Wang, X., Liang, X. Z., Jiang, W., Tao, Z., Wang, J. X. L., Liu, H., Han, Z., Liu, S., Zhang, Y., Grell, G. A., and Peckham, S. E.: WRF-Chem simulation of East Asian air quality: sensitivity to temporal and vertical emissions distributions, Atmos. Environ., 44, 660–669, 2010.

Wang, X., Wu, Z., and Liang, G.: WRF/CHEM modeling of impacts of weather conditions modified by urban expansion on secondary organic aerosol formation over Pearl River Delta, Particuology, 7, 384–391, 2009.

Yerramilli, A., Challa, V. S., Dodla, V. B. R., Dasari, H. P., Young, J. H., Patrick, C., Baham, J. M., Hughes, R. L., Hardy, M. G., and Swanier, S. J.: Simulation of Surface Ozone Pollution in the Central Gulf Coast Region Using WRF/Chem Model: Sensitivity to PBL and Land Surface Physics, Adv. Meteorol., 319138, https://doi.org/10.1155/2010/319138, 2010.

Ynoue, R. Y. and Andrade, M.: FSize-resolved mass balance of aerosol particles over the São 30 Paulo Metropolitan Area of Brazil, Aerosol Sci. Tech., 1, 52–62, 2004.

Zhang, D. and Anthes, R. A.: A High-Resolution Model of the Planetary Boundary Layer – Sensitivity Tests and Comparisons with SESAME-70 Data, J. Appl. Meteorol., 21, 1594–1609, 1982.

Zhang, H. L., Lia, J. Y., Ying, Q., Yu, J. Z., Wu, D., Cheng, Y., He, K. B., and Jiang, J. K.: Source apportionment of $PM_{2.5}$ nitrate and sulfate in China using a source oriented chemical transport model, Atmos. Environ., 62, 228–242, 2012.

Zhang, Q., Streets, D. G., Carmichael, G. R., He, K. B., Huo, H., Kannari, A., Klimont, Z., Park, I. S., Reddy, S., Fu, J. S., Chen, D., Duan, L., Lei, Y., Wang, L. T., and Yao, Z. L.: Asian emissions in 2006 for the NASA INTEX-B mission, Atmos. Chem. Phys., 9, 5131–5153, https://doi.org/10.5194/acp-9-5131-2009, 2009.

Zhou, D., Dai, Y., Yi, C., Guo, Y., and Zhu, Y.: China's sustainable energy scenarios in 2020, China Environmental Science Press, 2003.

Zhu, T., Melamed, M., Parrish, D., Gauss, M., Gallardo, L., Lawrence, M., and Knare, A.: Liousse. CWMO/IGAC Impacts of Megacities on Air Pollution and Climate, World Meteorological Organization Report No. World Meteorological Organization (WMO) Global Atmosphere Watch (GAW) Report No. 205, Geneva, 2013.